Jurnal Polimesin
Department of Mechanical Engineering
State Polytechnic of Lhokseumawe
http://e-jurnal.pnl.ac.id/polimesin
e-ISSN : 2549-1999 No. : 2 Month : April
p-ISSN : 1693-5462 Volume : 24 Year : 2026

Processing dates: received on 2026-1-23, reviewed on 2026-02-23, accepted on 2026-03-05 and online availability on 2026-04-25

Influence of cutting parameters on burr morphology in milling of 1–2 mm SS304 plates

Vian Rizanda Putra[1,*], Muhammad Akhlis Rizza[2]
[1]Applied Master's Program, Manufacturing Technology Engineering, State Polytechnic of Malang, Malang 65141, Indonesia
[2]Mechanical Engineering, State Polytechnic of Malang, Malang 65141, Indonesia
*Corresponding author: vian.rizanda.p@gmail.com

Abstract

Machining SS 304 in thin-plate applications presents a significant challenge due to burr formation arising from its high ductility and pronounced plastic deformation during milling. Within the 1 to 2 mm thickness range, reduced structural rigidity increases the tendency for lateral plastic flow and edge deformation, thereby compromising surface quality and increasing the need for secondary deburring operations. Although burr formation in stainless steel has been widely investigated, studies specifically addressing the influence of conventional milling parameters on burr morphology in thin SS 304 plates remain limited. This study aims to analyse the effects of spindle speeds (400 rpm and 800 rpm) and depth of cut (0.25 mm and 0.5 mm) on burr morphology in SS 304 plates with thicknesses of 1 mm, 1.5 mm, and 2 mm. Macroscopic observations were conducted using an optical microscope equipped with a 5× macro lens to evaluate burr height and deformation characteristics. The results demonstrate that increasing depth of cut consistently leads to higher burr formation due to intensified plastic deformation at the tool exit zone. Spindle speed contributes through thermomechanical effects that influence deformation stability, particularly in plates with differing rigidity. The 1 mm plate exhibited the highest burr value, reaching 284 µm, whereas the 2 mm plate showed more stable deformation behaviour with lower burr heights. These findings indicate that a combination of 800 rpm spindle speed and 0.25 mm depth of cut provides a more controlled burr condition, offering practical guidance for minimising burr defects in the conventional milling of thin SS 304 plates.

Keywords:
Burr formation, depth of cut, SS 304, spindle speed, thin plate milling.

1 Introduction

The SS 304 milling process is a fundamental stage in manufacturing, as it directly determines the dimensional precision, edge integrity, and surface quality of components and finished products. Among various machining methods, conventional milling is widely used to produce cutting tools fabricated from SS 304 plate, as well as other thin-plate mechanical support components [1], [2]. Although milling enables the generation of complex geometries with high accuracy, the process inevitably leads to burr formation along the exit edge of the workpiece [3]. The presence of burrs not only reduces product quality and increases dimensional deviation but also necessitates secondary operations such as deburring, thereby extending production time and increasing manufacturing costs. This issue becomes more critical in SS 304, a material widely used for its corrosion resistance and mechanical strength, yet characterised by high ductility that promotes significant plastic deformation during cutting [4].

Previous studies have investigated the influence of machining parameters, including spindle speed, feed rate, and depth of cut, on burr height and morphology in stainless steel machining [5]. The findings generally indicate that increasing the depth of cut tends to enlarge burr height due to the greater volume of material undergoing plastic deformation, while higher spindle speed affects the thermal conditions within the cutting zone, potentially intensifying or stabilising burr formation depending on the parameter combination. However, most existing research has focused on bulk materials or workpieces with relatively large thicknesses, where deformation behaviour is predominantly governed by shear mechanisms rather than structural deflection effects [6].

In current industrial applications, the use of thin SS 304 plates with thicknesses ranging from 1 to 2 mm has become increasingly common, particularly in lightweight, precision-engineered components. Within this thickness range, material rigidity becomes a dominant factor influencing lateral plastic flow and deformation stability as the cutting tool exits the workpiece. Thinner plates are more susceptible to deflection and bending, which may intensify roll-over burr formation and lateral deformation associated with transverse strain effects [7], [8].

Despite this, systematic investigations linking thin-plate thickness variations between 1 and 2 mm with combinations of spindle speed and depth of cut in conventional milling remain limited. Furthermore, the rationale for parameter selection is often insufficiently justified in relation to practical industrial conditions. The plate thicknesses of 1.0 mm, 1.5 mm, and 2.0 mm selected in this study correspond to commonly utilised SS 304 plate dimensions in thin-component manufacturing using conventional milling processes. The spindle speed range of 400-800 rpm was chosen to represent actual operating conditions frequently used in conventional milling machines equipped with a 12 mm diameter end mill [9]. These speeds are widely used in industrial practice and are often associated with burr formation during SS 304 plate machining. Moreover, this range allows evaluation of thermomechanical responses at low-to-moderate speeds without entering the domain of high-speed machining, thereby ensuring practical industrial relevance [10], [11].

Based on these considerations, this study aims to systematically analyse the influence of spindle speed and depth of cut on burr morphology in thin SS 304 plates with thicknesses of 1-2 mm, and to elucidate the underlying deformation mechanisms. The investigation not only quantitatively evaluates burr height but also examines morphological characteristics and deformation orientation through macroscopic observation with an optical microscope. Accordingly, this study seeks to address the existing research gap and provide both scientific insight and practical guidance for optimising conventional milling parameters in order to minimise burr defects in thin SS 304 plate applications [12], [13].

2 Methods and materials

This study adopted a laboratory-based experimental approach to examine the influence of machining parameters on burr defect characteristics in SS 304 plates. The specimens comprised SS 304 plates with thicknesses of 1 mm, 1.5 mm, and 2 mm. Machining was performed using a conventional milling process with a 12 mm diameter end mill cutter. The cutting parameters investigated were spindle speeds of 400 rpm and 800 rpm, together with depths of cut of 0.25 mm and 0.5 mm [14]. Each parameter combination produced distinct burr features along the machined edges of the SS 304 plates. The burr defects formed during the milling process were subsequently characterised through controlled macroscopic examination to assess their morphology, geometry, and surface characteristics. This experimental framework enabled a systematic evaluation of the relationship between plate thickness and cutting

parameters in determining the severity and morphological attributes of the burrs generated [15].

2.1 Material and milling process

The material for this research is SS 304 plate with varying thicknesses, cut into 450 mm × 100 mm specimens. This SS 304 plate material contains less than 0.08% carbon (C). Increasing the carbon content can reduce corrosion resistance, so the SS 304 plate material is rust-resistant and ductile [16]. The SS 304 plate material that has been cut according to the dimensions adjusted by the milling process is carried out by clamping the specimen on a jig fixture with cutting depth variation parameters of 0.25 and 0.5 mm and spindle speed of 400 rpm and 800 rpm, so that the morphology of burr defects can be clearly represented. The SS 304 plate specimen is shown in Fig. 1 [17].

The milling process is carried out in several stages, beginning with the preparation of test materials, namely SS 304 plates as shown in the Fig. 1. After the material preparation process is complete, the next stage is the milling process, which is carried out in accordance with the preparation scheme and work procedures represented in Fig. 2. This stage includes determining the workpiece position, adjusting cutting parameters, and using jigs and fixtures to ensure stable, accurate machining [17].

This milling process began by preparing test specimens in the form of SS 304 plates cut to standard dimensions. The specimens were then clamped to the milling machine table using a jig to ensure stability during milling. Cutting was performed using a 12 mm-diameter end mill cutter, as shown in the research equipment diagram. The machining parameters used were spindle speeds of 400 and 800 rpm and cutting depths of 0.25 mm and 0.5 mm, respectively [18]. This combination of parameters was selected to analyse the effect of cutting conditions on the surface quality of the machining results. After the milling process was completed, the specimens were tested to measure and analyse the burr defects formed at the cut edges. Measurements were taken using precision measuring instruments and an optical microscope to obtain accurate images of the surface details and burr sizes. The observation data were then used to evaluate the effects of machining parameter variations on burr defect formation and the surface characteristics of SS 304 plate material [19].

Fig. 1. SS 304 plate specimens.

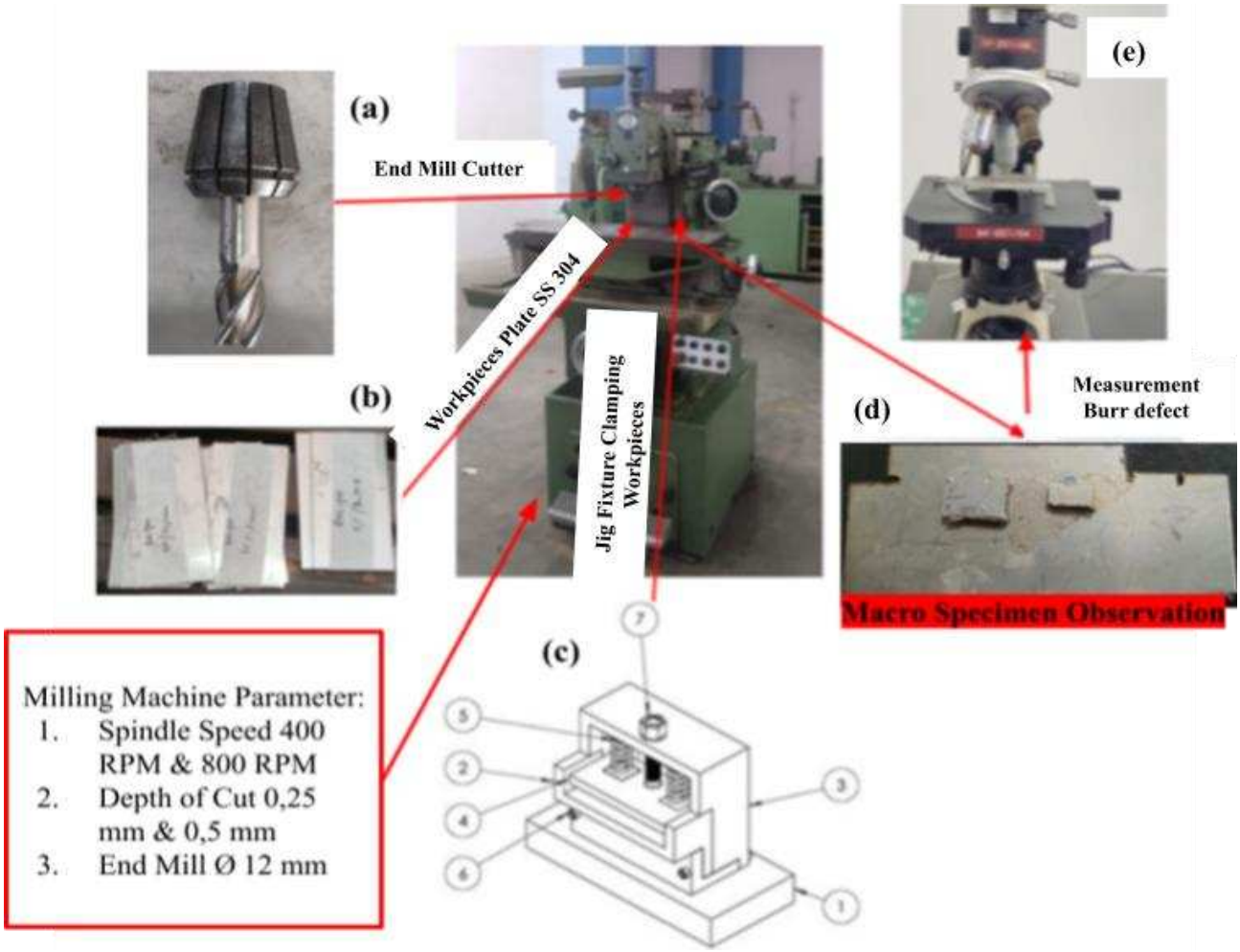

Fig. 2. Experimental setup of the conventional milling process. (a) End mill cutter 12 mm, (b) plate SS 304, (c) jig fixture, (d) specimen macro observation, (e) optical microscope.

2.2 Macro measurement preparation

Upon completion of the milling operation, the specimens were subjected to surface characterisation by means of macroscopic analysis. This examination aimed to assess and characterise burr defects along the edges of SS 304 plates. The observations were conducted using an optical microscope fitted with a 5× macro lens. The corresponding macroscopic images are presented in Fig. 3 [20].

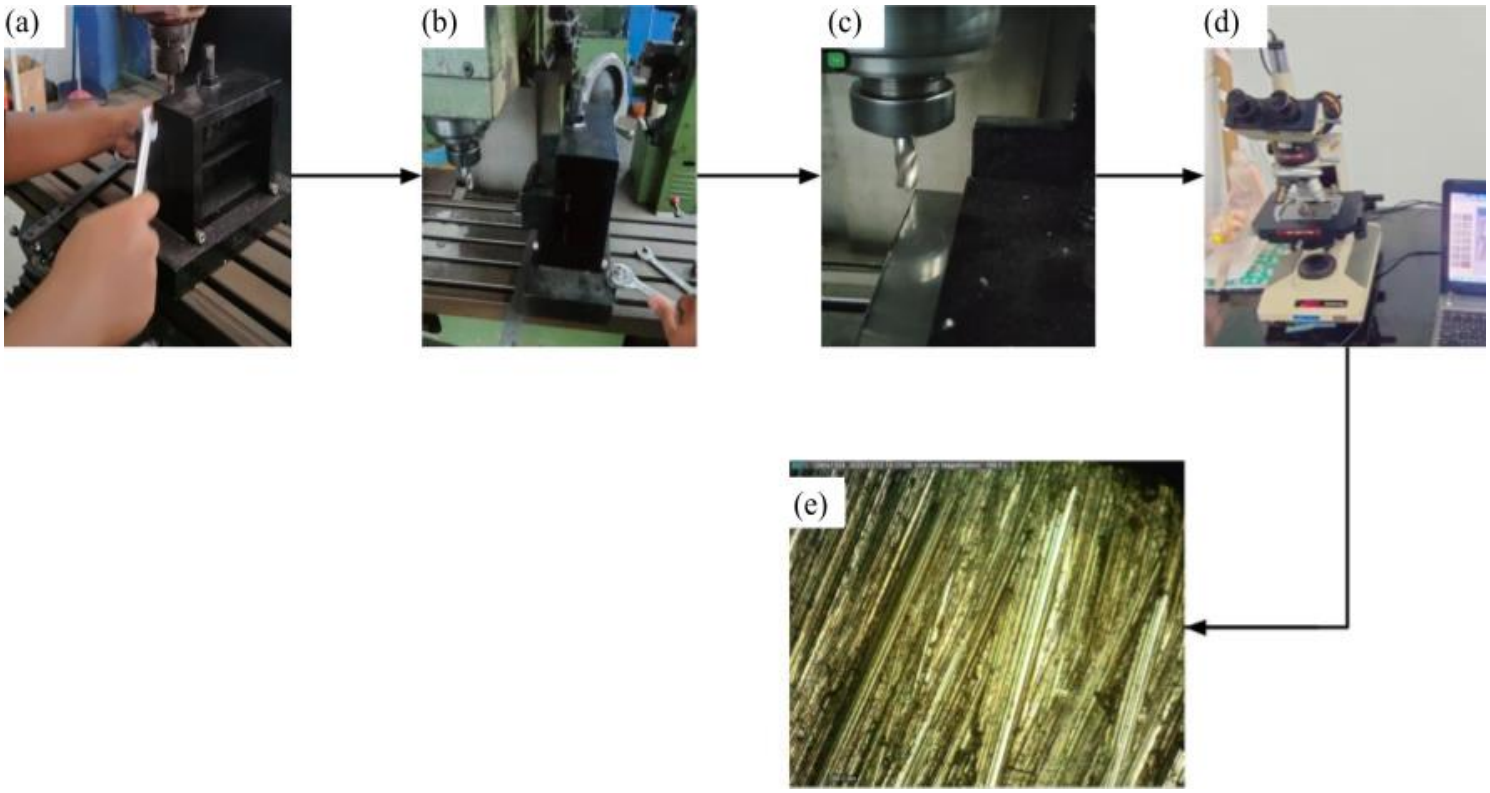

Fig. 3. Macroscopic observation setup for burr defect characterization. (a) Clamp element, (b) setup milling, (c) machining process, (d) measurement burr defect, (e) burr characterization.

The initial stage involved sectioning SS 304 plate stock using a precision-cutting machine to obtain test specimens with dimensions compliant with the specified standards. The specimens were subsequently secured on a conventional milling machine using a dedicated jig fixture to ensure positional stability during machining under predetermined experimental parameters. The next stage comprised surface milling to generate the designated test area and produce the required surface characteristics. Following machining, the samples were examined using an optical microscope equipped with a macro lens to identify alterations in surface structure induced by the cutting process [21]. The final image presents the observed microstructural features, highlighting the scratch patterns and the material flow orientation resulting from the interaction between the cutting tool and the workpiece.

2.3 Test procedure

The experiments were conducted using SS 304 plates as test specimens, with thicknesses of 1 mm, 1.5 mm, and 2 mm to evaluate the influence of thickness on burr formation. The machining parameters applied in this study included spindle speeds of 400 and 800 rpm, along with depths of cut of 0.25 mm and 0.5 mm. The combination of plate thickness variations and cutting parameters was designed to enable a comprehensive comparison of the contribution of each variable to the characteristics of the burr defects produced [22]. The feed rate was determined in accordance with the Eq. (1).

$$fr = f \times N \tag{1}$$

The Material Removal Rate (MRR) formula is used to calculate the rate of material removal after milling a 304 SS plate specimen [22], [23], as written in the Eq. (2).

$$MRR = f \times d \times Vc \tag{2}$$

The research process began with the preparation of test materials, namely SS 304 plates, which were cut to standard sizes using a fibre laser cutting machine to obtain uniform specimen dimensions [24]. After cutting, jig fixtures were made and adjusted to hold the workpiece on the milling machine, ensuring the specimen remained stable during machining. The next stage involved determining the position and clamping of the SS 304 plates on the milling machine's jig fixture [25]. The milling process was carried out with varying parameters, including spindle speed, feed rate, and cutting depth. After machining, the specimens were tested for straightness and surface dimensions using precision measuring instruments to ensure compliance with design tolerances [26]. Macroscopic observation of the machined surface is performed using an optical microscope connected to a computer device [27]. This observation aims to analyse the surface structure, scratch direction, and morphological changes due to variations in machining parameters. The observation images are then enlarged to obtain a detailed picture of the surface topography, which serves as the primary data for analysing roughness and machining characteristics [28] (Fig. 4).

3 Results and discussion

This milling process experiment on SS 304 plates was designed to produce data that is not only numerical but also systematically organised to facilitate analysis of the relationships between machining process parameters, variations in workpiece thickness, and the mechanical behaviour observed in the machining results. The analysis was conducted based on the surface morphology of the cut results, so that the results and discussion sections not only display the maximum burr defect values but also explain the relationship between the workpiece thickness and variations in machining parameters on surface characteristics. The analysis approach is presented through a comparison graph of the maximum and average values of each SS 304 specimen replication [29]. This visualisation allows interpretation of the direct relationship between the combination of machining parameters and workpiece thickness and burr defect formation. The use of plate thickness variations in this study aims to update the findings of previous studies with similar experimental configurations. This study used a conventional milling machine with a jig fixture to ensure the stability and precision of the specimen position during cutting. After machining, the specimen was tested using surface macrophotography to measure and identify the burr heights formed. The macro observation results are shown in Fig. 5-Fig. 7, which details the surface morphology of the machined specimen [30].

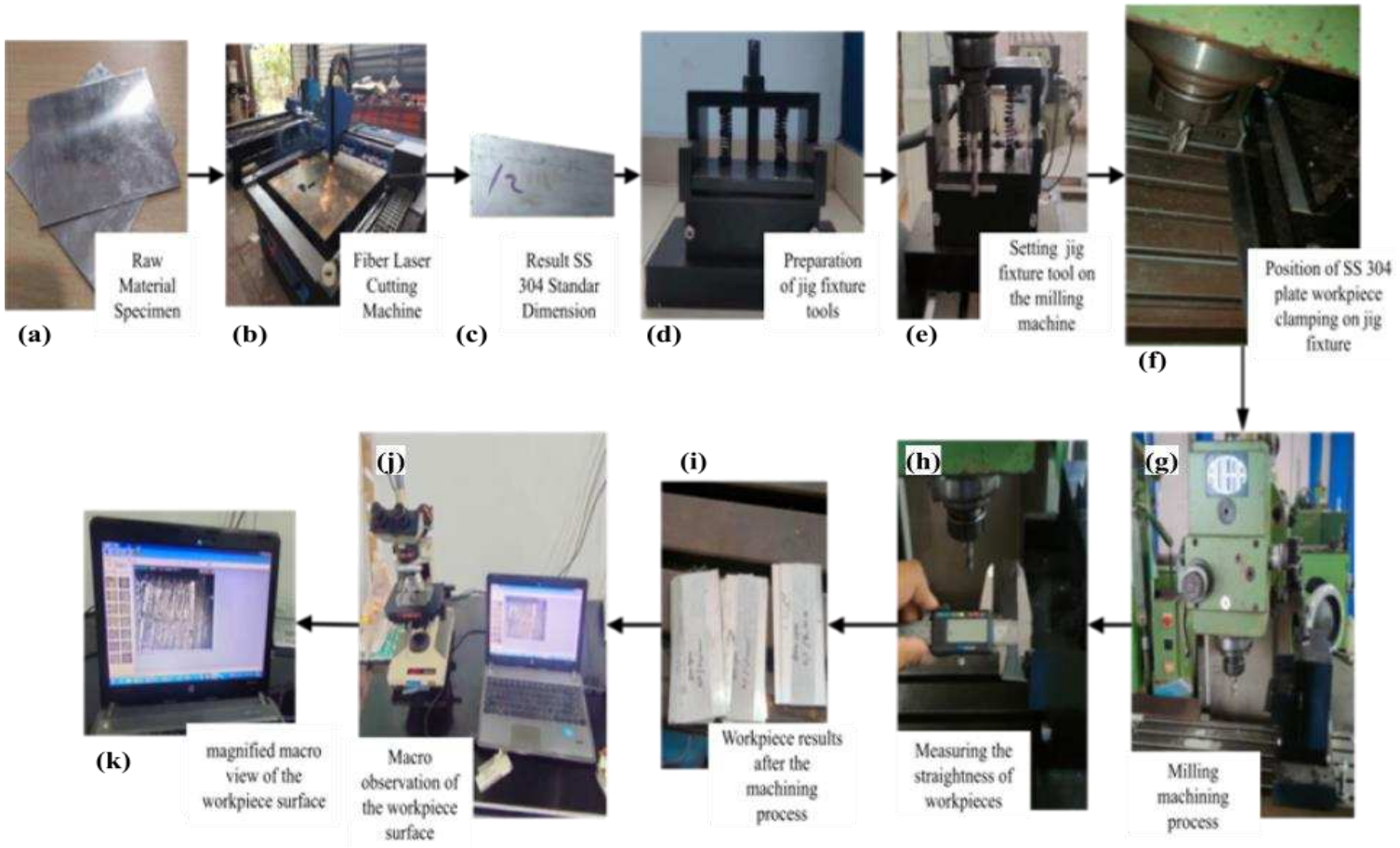

Fig. 4. Preparation stage for burr measurement on SS 304 plates. (a) Raw material, (b) laser cutting, (c) specimen SS 304, (d) jig fixture, (e) setting jig fixture, (f) clamping element, (g) milling process, (h) measure position, (i) specimen result, (j) macro observation, (k) magnified macro view.

Macroscopic observations of the 1 mm thick SS 304 plates indicate that variations in spindle speed and depth of cut directly influence the resulting burr morphology. At 400 rpm with a depth of cut of 0.25 mm (Fig. 5(a)), the burrs formed are relatively small and unevenly distributed, while the machining marks remain clearly visible, suggesting limited plastic deformation at the exit edge. Increasing the depth of cut to 0.5 mm at the same spindle speed (Fig. 5(b)) leads to a marked increase in burr height and thickness, attributable to the greater volume of material undergoing plastic shearing and bending at the tool exit zone [31]. At 800 rpm with a depth of cut of 0.25 mm (Fig. 5(c)), the burrs appear thinner yet more elongated along the feed direction, indicating that elevated cutting temperatures promote material softening and facilitate plastic flow. The combination of 800 rpm and a depth of cut of 0.5 mm (Fig. 5(d)) produce the most pronounced burr formation, characterised by a denser structure and more directional deformation. This condition reflects the combined effect of increased mechanical loading and intensified thermal influence [32]. Overall, increasing the depth of cut consistently amplifies burr formation, while higher spindle speeds, under certain conditions, further exacerbate burr development due to thermomechanical interactions in the cutting zone. These findings highlight the critical importance of controlling machining parameters to maintain edge quality when milling thin SS 304 plates [33].

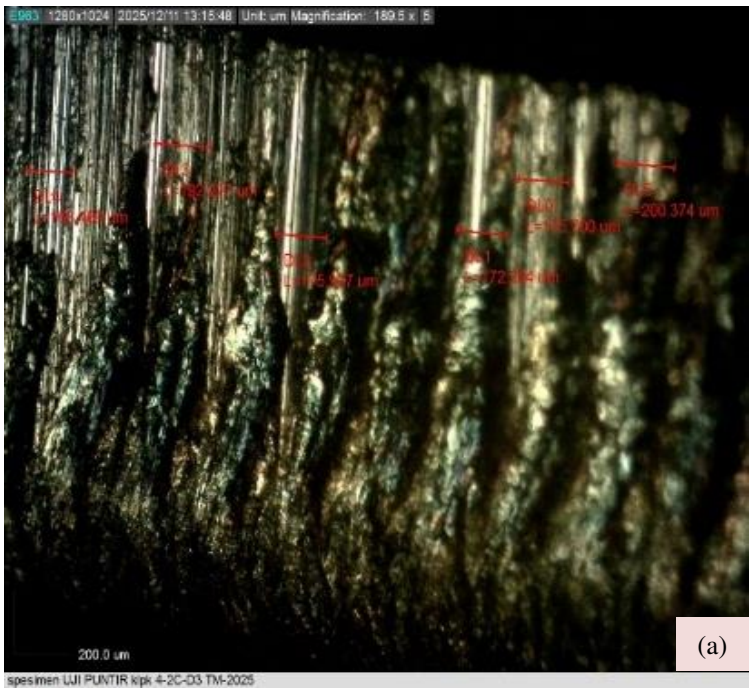

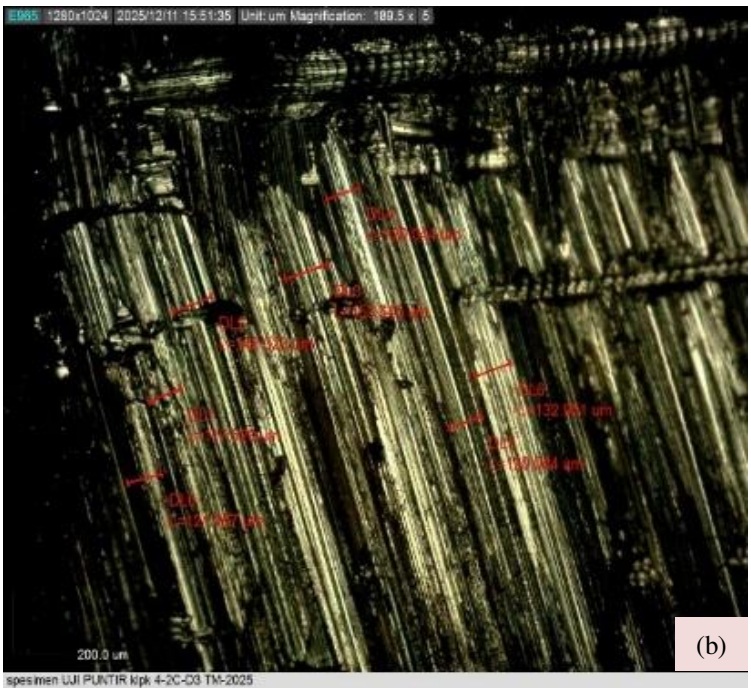

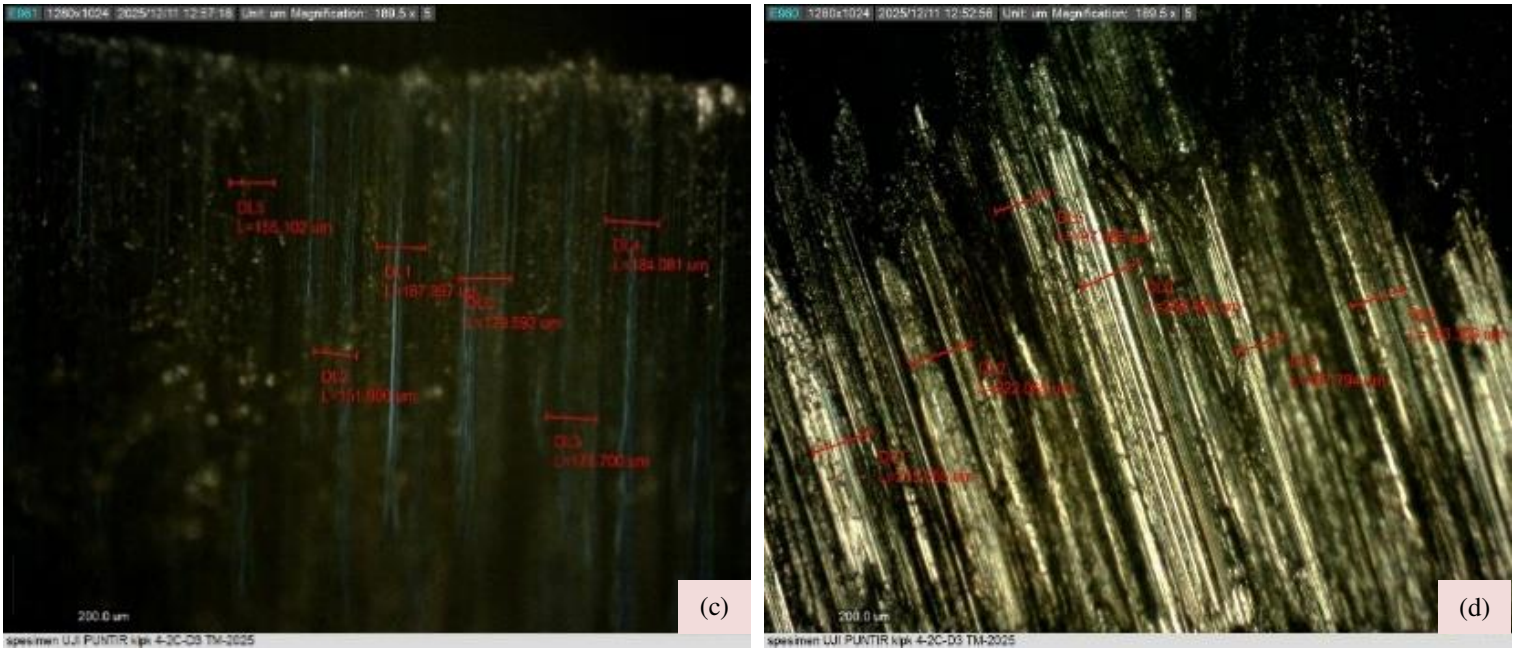

Fig. 5. Plates thickness 1 mm macro burr defect measurement. (a) 400 rpm depth cut 0.25 mm, (b) 400 rpm depth cut 0.5 mm, (c) 800 rpm depth cut 0.25 mm, (d) 800 rpm depth cut 0.5 mm.

Macroscopic observations of the 1.5 mm thick SS 304 plates reveal a burr formation pattern distinct from that observed in the 1 mm plates, particularly in terms of burr density and deformation orientation. At 400 rpm with a depth of cut of 0.25 mm (Fig. 6(a)), the burrs appear relatively stable, exhibiting a wavy profile aligned with the cutting tool path. The burr height remains limited, suggesting that the combined effect of moderate mechanical loading and increased plate thickness provides greater resistance to excessive deformation at the exit edge. When the depth of cut is increased to 0.5 mm at the same spindle speed (Fig. 6(b)), a noticeable rise in burr height and thickness is observed, accompanied by material accumulation along the cut edge [34]. The machining marks become deeper and more closely spaced, indicating higher cutting forces and more pronounced plastic deformation. At 800 rpm with a depth of cut of 0.25 mm (Fig. 6(c)), the burrs tend to be more elongated and oriented along the feed direction, with a comparatively smoother surface texture. This behaviour reflects the contribution of thermal effects, which enhance material plasticity and facilitate plastic flow at the edge [35]. The combination of 800 rpm and a depth of cut of 0.5 mm (Fig. 6(d)) produce the most prominent burr morphology, characterised by thicker, denser structures and more uniform plastic deformation along the edge. These observations confirm that increasing the depth of cut remains the primary factor in intensifying burr formation, while higher spindle speeds further reinforce this effect through thermomechanical interaction. Overall, at a thickness of 1.5 mm, the plate exhibits a more controlled deformation response compared with the 1 mm specimen; however, the tendency for burr enlargement with increasing machining parameters remains consistent [36].

Macroscopic observations of the 2 mm-thick SS 304 plates indicate more controlled burr characteristics than those of the 1 mm and 1.5 mm specimens, reflecting the increased structural rigidity of the thicker material against edge deformation. At 400 rpm with a depth of cut of 0.25 mm (Fig. 7(a)), the burrs formed are relatively thin and uniform, with clearly visible machining marks and minimal material accumulation at the exit edge. This suggests that the combination of lower mechanical loading and greater plate thickness effectively limits excessive plastic deformation [35]. Increasing the depth of cut to 0.5 mm at 400 rpm (Fig. 7(b)) results in a measurable rise in burr height, although its distribution remains relatively stable.

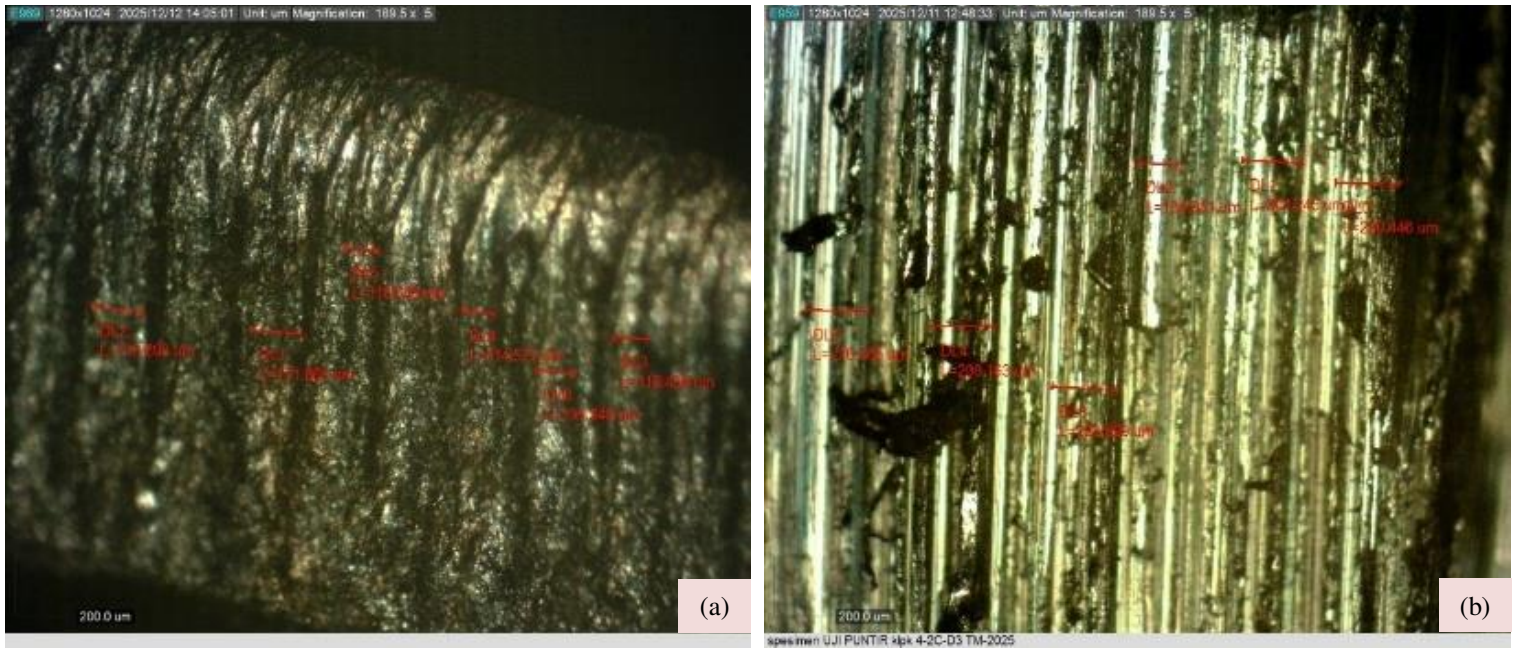

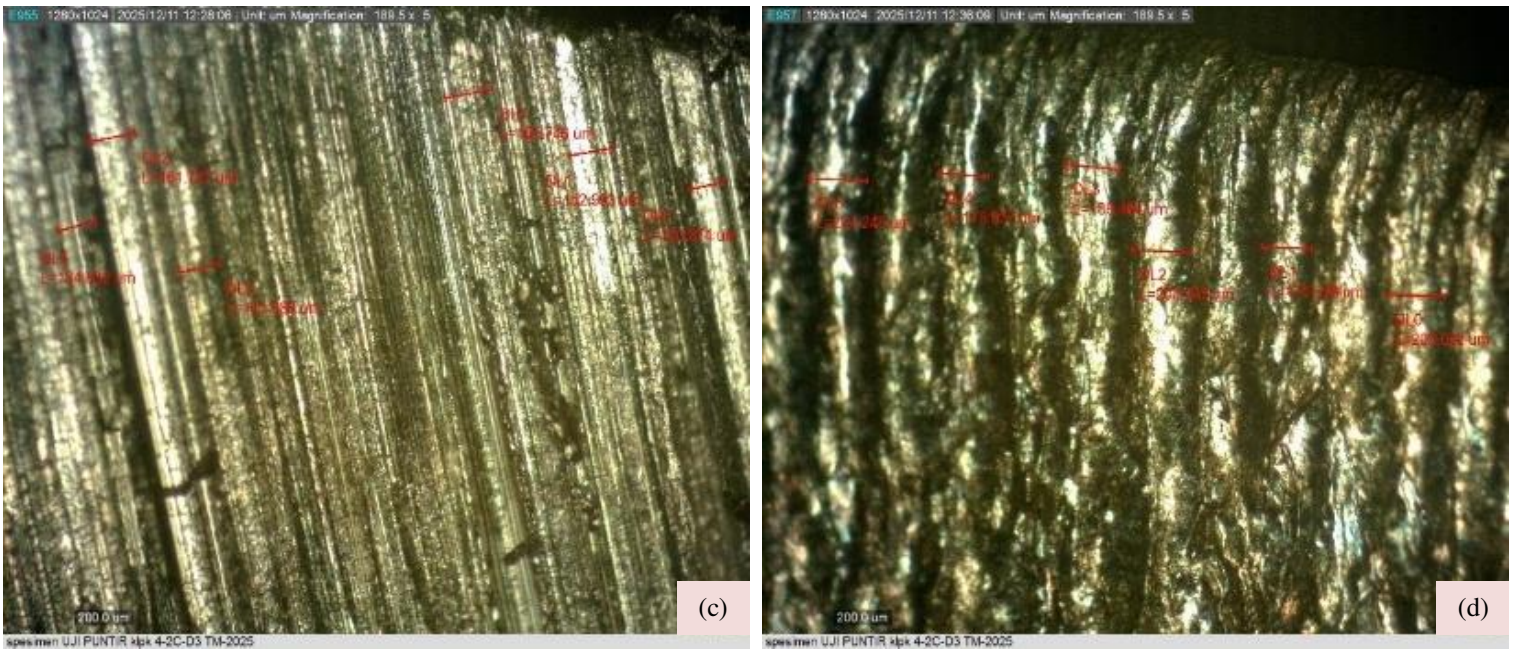

Fig. 6. Plates thickness 1.5 mm macro burr defect measurement. (a) 400 rpm depth cut 0.25 mm, (b) 400 rpm depth cut 0.5 mm, (c) 800 rpm depth cut 0.25 mm, (d) 800 rpm depth cut 0.5 mm.

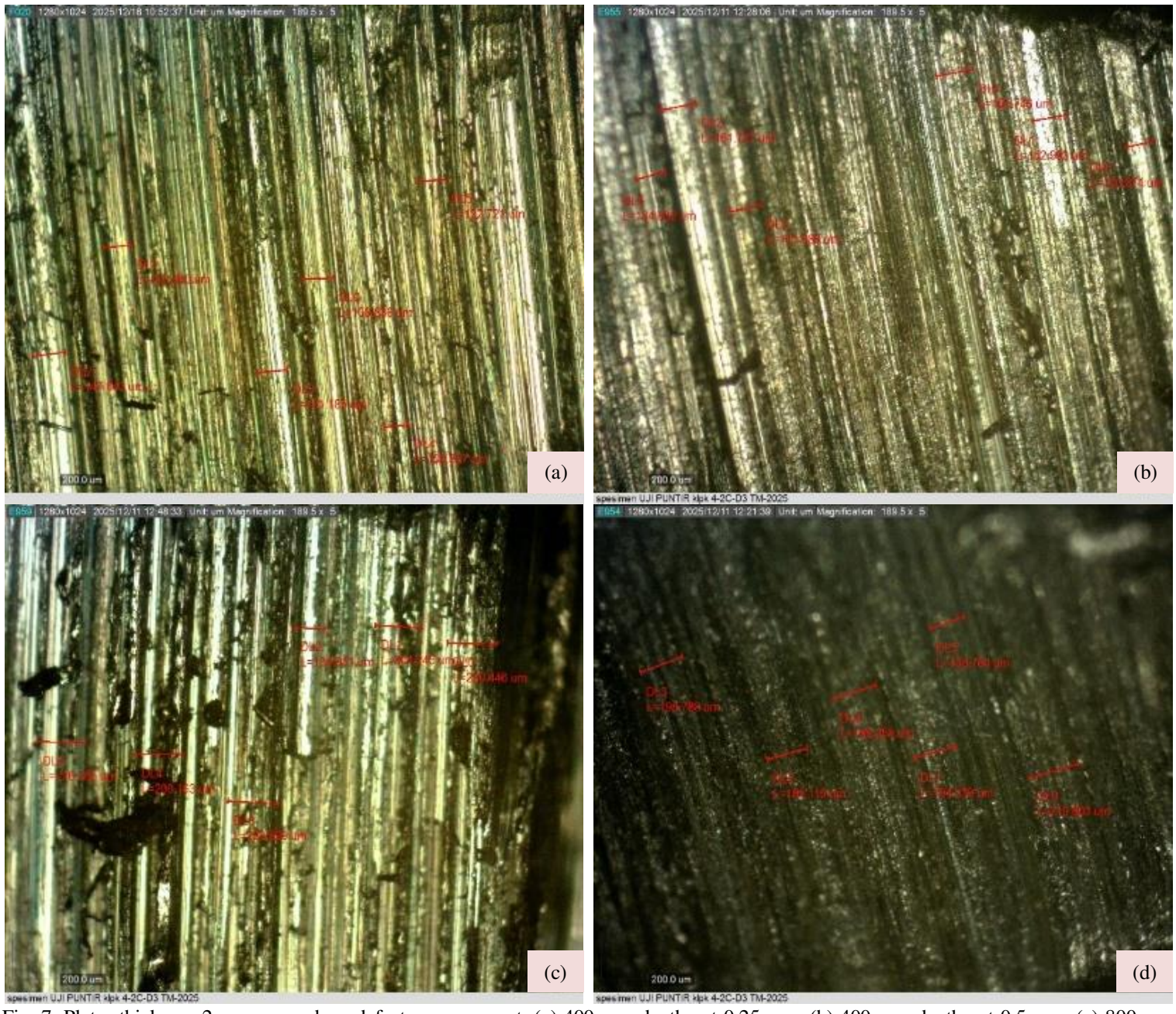

Fig. 7. Plates thickness 2 mm macro burr defect measurement. (a) 400 rpm depth cut 0.25 mm, (b) 400 rpm depth cut 0.5 mm, (c) 800 rpm depth cut 0.25 mm, (d) 800 rpm depth cut 0.5 mm.

Localised thickening at certain edge regions indicates higher shear forces and intensified plastic flow. At 800 rpm with a depth of cut of 0.25 mm (Fig. 7(c)), the burrs tend to elongate along the cutting direction, suggesting a thermal contribution that enhances material plasticity without inducing excessive deformation. The combination of 800 rpm and a depth of cut of 0.5 mm (Fig. 7(d)) produce the most pronounced burr morphology at this thickness, characterised by increased burr height and denser deformation structures along the cut edge. Nevertheless, compared with thinner plates, deformation in the 2 mm specimen remains more controlled and does not exhibit severe folding. Overall, these findings confirm that increasing the depth of cut consistently intensifies burr formation, while higher spindle speeds further reinforce this effect through thermomechanical contributions. However, greater plate thickness provides a stabilising effect on edge deformation, resulting in relatively lower burr severity than that observed in thinner specimens [36].

3.1 Result macro measurement

Macro measurements were taken on the surfaces of SS 304 plate workpieces that had undergone milling to evaluate morphological characteristics arising from variations in machining parameters and plate thickness. Three thickness variations (1 mm, 1.5 mm, and 2 mm), two spindle speeds (400 rpm and 800 rpm), and two cutting depths (0.25 mm and 0.5 mm) were tested. This experimental design aimed to examine the effect of geometric factors and operating parameters on the resulting surface morphology [37]. The evaluation of these macro measurements is intended to represent the surface-morphology response of SS 304 workpieces to changes in machining conditions and to determine the optimal combination of parameters and material thickness for producing the best surface characteristics. The maximum measurement results for all parameters used are presented in Table 1, which compares surface features for each machining condition [38].

Table 1 shows the results of macro measurements of the maximum burr defect value on the surface of SS 304 plate specimens for various combinations of workpiece thickness, cutting depth, and spindle speed. This test aims to understand the effect of machining parameters on the morphological characteristics of the milling process surface. At a spindle speed of 400 rpm, increasing the cutting depth from 0.25 mm to 0.5 mm tends to increase the maximum burr value across all specimen thicknesses. For example, for a thickness of 1 mm, the maximum value increased from 180.104 µm to 237.297 µm, while for a thickness of 2 mm, the maximum value increased from 150.523 µm to 160.849 µm [39], [40]. This pattern indicates that the greater the cutting depth, the higher the cutting energy produced, thereby increasing plastic deformation at the cutting edge and forming larger burrs. When the spindle speed is increased to 800 rpm, a different trend is observed. In general, increasing the cutting depth continues to increase burr formation, but some values show a decreasing trend, particularly at larger specimen thicknesses. As an example of the results, for the 2 mm specimen, the maximum value decreased from 162.122 µm at a depth of 0.25 mm to 147.843 µm at a depth of 0.5 mm [41].

Table 1. Data collection 1st test

Specimen thickness (mm)	Depth of cut (mm)	Spindle speed (rpm)	Max value (µm)
1	0.25	400	180.104
	0.5		237.297
1.5	0.25	400	188.861
	0.5		204.978
2	0.25	400	150.523
	0.5		160.849
1	0.25	800	284.253
	0.5		184.081
1.5	0.25	800	219.803
	0.5		165.746
2	0.25	800	162.122
	0.5		147.843

This indicates that increasing the spindle speed can improve cutting efficiency, reduce shear forces and local heat, thereby inhibiting the formation of excessive burrs at the cutting edge. When viewed in terms of specimen thickness, it can be observed that materials with thicknesses less than 1 mm generally produce higher burr values than thicker specimens. This phenomenon is related to the material's rigidity. At thinner thicknesses, the workpiece experiences greater deflection during the cutting process, which then increases plastic deformation at the edge. Overall, the results in Table 1 show that the combination of a high spindle speed of 800 rpm and a small cutting depth of 0.25 mm provides the most stable machining results with relatively low burr formation. These conditions can be recommended as the optimum parameters for producing machined surfaces with better morphological quality on SS 304 material. The data in the Table 1 are shown in the graph in Fig. 8 [42].

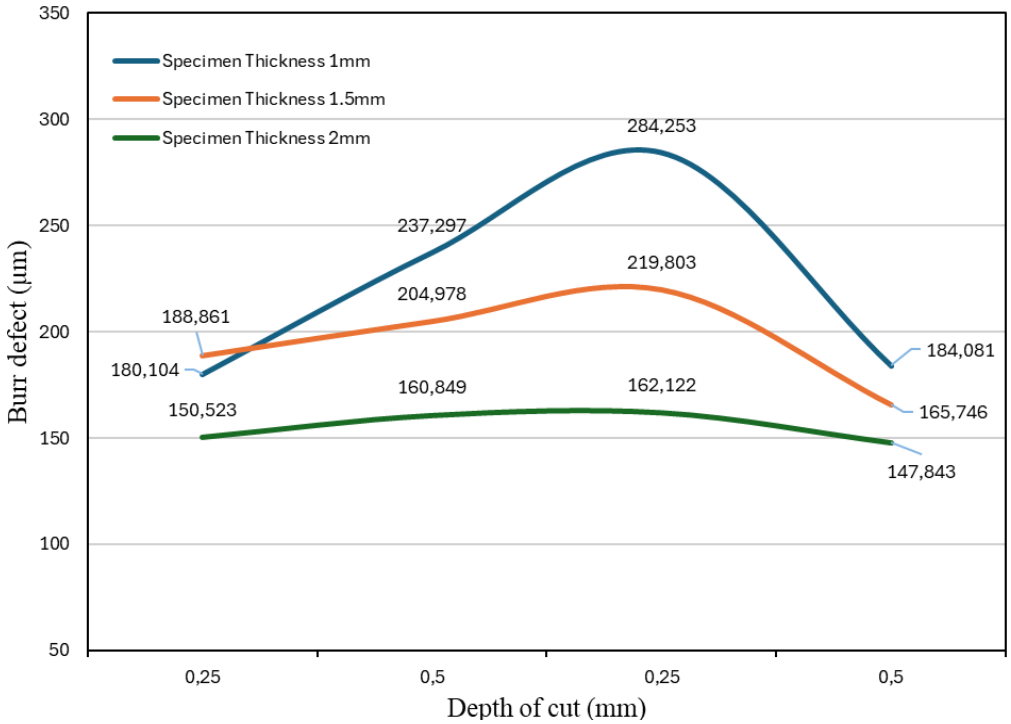

Fig. 8. Graph analysis 1st test.

Fig. 8 shows the relationship between cutting depth and maximum burr value for three SS 304 specimen thicknesses: 1 mm, 1.5 mm, and 2 mm. This graph is a visual representation of the data in Table 1 and illustrates the trend of surface morphology changes due to variations in machining conditions. It is clear that, for all specimen thicknesses, the maximum burr value increases with increasing cutting depth up to a certain point, then decreases again at a higher spindle speed of 800 rpm. In specimens with a thickness of 1 mm, the burr value increased sharply from 180.104 µm to 284.253 µm, the highest value among all machining conditions. This indicates that thin specimens are less rigid, making them more susceptible to plastic deformation and the formation of larger burrs as the cutting depth increases [43], [44]. Meanwhile, at a thickness of 1.5 mm, an increase in cutting depth from 0.25 mm to 0.5 mm resulted in relatively more stable changes, with maximum burr values ranging from 204.978 µm to 219.803 µm. These conditions indicate that at medium thickness, there is a balance between material rigidity and cutting force, so that burr formation still occurs but less than in specimens with thinner thicknesses. Conversely, specimens with a thickness of 2 mm showed the lowest burr values and tended to remain stable across all cutting depths [45].

The maximum value ranged from 147.843 µm to 162.122 µm, indicating that an increase in specimen thickness provided better rigidity against cutting forces, thereby minimising plastic deformation at the cutting edge. The downward trend in burr values at a depth of cut of 0.5 mm and a spindle speed of 800 rpm across all specimens indicates that high spindle speed reduces burr formation. This is due to increased cutting efficiency and reduced friction between the cutter and the material, thereby reducing the deformation energy transferred to the cutting zone [46]. Overall, the results in Fig. 8 show that the combination of a high spindle speed of 800 rpm and a small cutting depth of 0.25 mm produces the best surface condition, with the lowest burr values. These findings confirm the pattern obtained in Table 1 and reinforce the results that control of machining parameters has a significant effect on the surface quality and morphology of milling results on SS 304 material. The replication results are represented in Table 2 [47].

Table 2. Data collection 2nd test

Specimen thickness (mm)	Depth of cut (mm)	Spindle speed (rpm)	Max value (µm)
1	0.25	400	153.645
	0.5		223.299
1.5	0.25	400	176.693
	0.5		228.843
2	0.25	400	147.843
	0.5		134.867
1	0.25	800	200.374
	0.5		222.065
1.5	0.25	800	165.746
	0.5		204.245
2	0.25	800	226.899
	0.5		225.864

Table 2 shows the macro measurement results in the second test for SS 304 specimens with variations in workpiece thickness, cutting depth, and spindle speed. The purpose of this test was to ensure the consistency of the results obtained in the first replication and to assess the stability of burr formation behaviour against changes in machining conditions [17]. At a spindle speed of 400 rpm, increasing the cutting depth from 0.25 mm to 0.5 mm generally increased the maximum burr value for each specimen thickness. At a thickness of 1 mm, the burr value increased from 153.645 µm to 223.299 µm, while at 1.5 mm, the maximum value increased from 176.693 µm to 228.843 µm. This indicates that increasing cutting depth increases the volume of material removed by the cutter, resulting in higher shear stress and plastic deformation at the cutting edge. Interestingly, for specimens 2 mm thick, a slightly different pattern is observed. The maximum burr value actually decreased from 147.843 µm at a depth of 0.25 mm to 134.867 µm at a depth of 0.5 mm. This indicates that at a certain thickness, an increase in cutting depth can stabilise the cutting force because the workpiece's higher rigidity resists local deformation, thereby reducing burr formation. When the spindle speed was increased to 800 rpm, the trend that emerged showed a more complex pattern. On the 1 mm specimen, the maximum burr value reached 222.065 µm, with slight fluctuations compared to the results at 400 rpm [48].

This condition indicates that increasing spindle speed does not completely eliminate burrs, but it can reduce the severity of deformation by accelerating material release in the cutting zone. For the 1.5 mm specimen, the maximum burr value ranged from 165.746 µm to 204.245 µm, indicating good stability against variations in cutting depth. However, the most significant results were seen at a thickness of 2 mm, where the maximum burr values increased sharply to 226.899 µm and 225.864 µm [49]. This phenomenon indicates that, with a combination of high spindle speed and thicker material, local heat accumulation and increased lateral cutting forces occur, which encourage the formation of larger burrs at the cutter exit. Overall, the results of the second replication showed a pattern consistent with the first replication, with differences in values still within the reasonable range of variation. It can be concluded that the spindle speed and cutting depth parameters have a dominant influence on the height of the burr formed, while the thickness of the specimen plays a role in determining the stability of material deformation during the cutting process [50], [51]. These results indicate that for SS 304 material, the combination of high speed 800 rpm and low cutting depth 0.25 mm remains the most effective condition in minimising burr formation while maintaining the dimensional stability of the machining results [27]. The data in Table 2 is represented in the form of a graph shown in Fig. 9.

Fig. 9 shows the relationship between depth and the maximum burr value for SS 304 plate specimens with three thicknesses: 1 mm, 1.5 mm, and 2 mm. This graph visually represents the data in Table 2 and provides a comprehensive overview of the effects of machining parameter variations on changes in the morphological characteristics of the milled surface. The graph shows that each specimen thickness exhibits a different pattern in response to changes in cutting depth and spindle speed. In specimens with a thickness of 1 mm, the burr value increased significantly when the cutting depth increased from 0.25 mm to 0.5 mm, namely from 153.645 µm to 223.299 µm. This indicates that an increase in cutting depth on thin materials results in greater plastic deformation due to the low rigidity of the workpiece, causing higher burrs to form on the cutting edge [52]. In the 1.5 mm specimen, the pattern that emerged showed that burrs reached a maximum value of 228.843 µm at a cutting depth of 0.5 mm and a spindle speed of 400 rpm, then decreased at 800 rpm under the same cutting depth conditions. This phenomenon indicates that increasing the spindle speed can reduce friction and local temperature, thereby controlling the deformation energy in the cutting zone. As a result, burr formation decreases even though the cutting depth remains high. Meanwhile, the 2 mm thick specimen exhibited different behaviour compared to the other two specimens. At a cutting depth of 0.25 mm, the burr value was relatively small at 147.843 µm but increased dramatically to 226.899 µm at a spindle speed of 800 rpm [53].

This phenomenon indicates that, in thicker materials, lateral cutting forces increase with spindle speed. This condition results in greater heat accumulation and increased shear forces on the tool's exit side, leading to larger burrs. In general, the graph shows that workpiece thickness directly affects deformation stability during cutting. Thicker materials (2 mm) tend to resist deformation better at low cutting depths, but produce higher burrs when the spindle speed increases due to increased cutting forces. Conversely, thinner materials show a significant increase in burrs even at small cutting depths, due to their lower rigidity. The correlation between the results in Table 2 and this graph reinforces the experimental results that the combination of a high spindle speed of 800 rpm with a low cutting depth of 0.25 mm is the most effective machining condition

for minimising burr formation on SS 304 plate material [54], [55]. This finding also confirms that machining parameters have an interdependent influence on edge deformation behaviour, where an increase in one variable must be accompanied by adjustments to other variables to maintain stable thermal and mechanical cutting results [56].

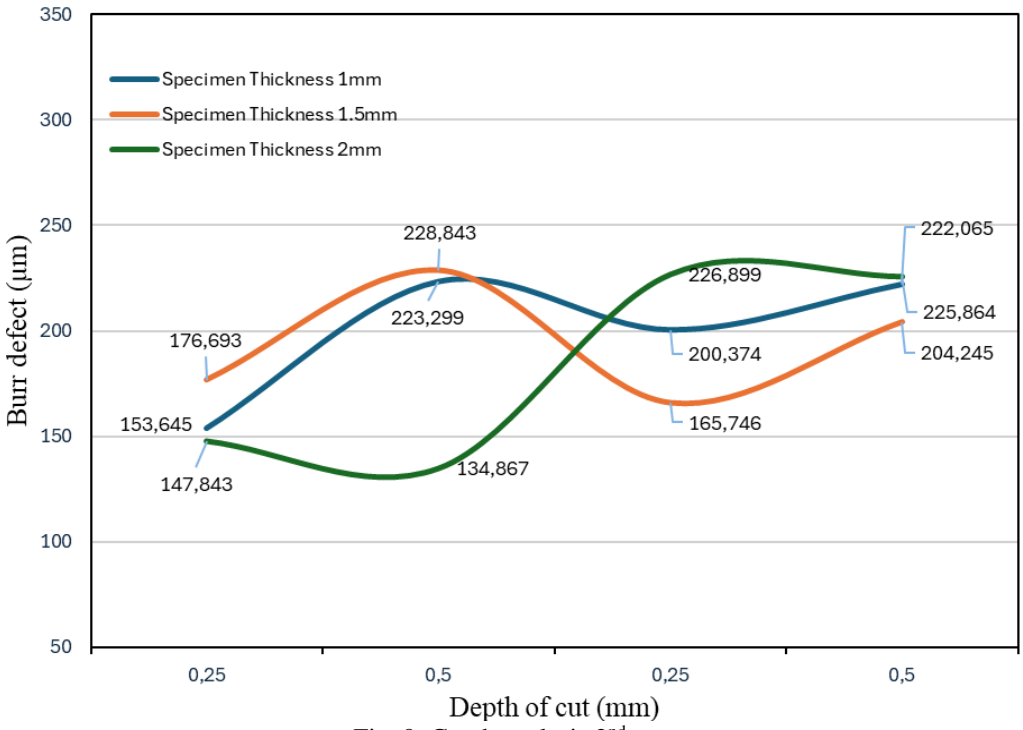

Fig. 9. Graph analysis 2nd test.

3.2 Schematic burr formation

Fig. 10 illustrates the schematic mechanism of burr formation in ductile SS 304 plates through the evolution of deformation zones at the tool exit region. In the initial stage, the interaction between the cutting tool and the workpiece generates a primary shear zone accompanied by elastoplastic deformation around the tool tip. As the tool approaches the workpiece edge, the plastic zone expands and strain concentration increases as material constraint progressively decreases [57]. This change in boundary conditions leads to a redistribution of stresses from predominantly shear to a combined shear–tensile state at the free surface, thereby promoting lateral plastic flow prior to complete chip separation [58], [59]. In highly ductile materials such as SS 304, fracture does not occur in a brittle manner; instead, it is preceded by substantial plastic deformation around a pivot point at the tool exit side [60]. The development of a negative shear zone intensifies the strain gradient and delays crack propagation, leading to partial material folding and the formation of a roll-over burr.

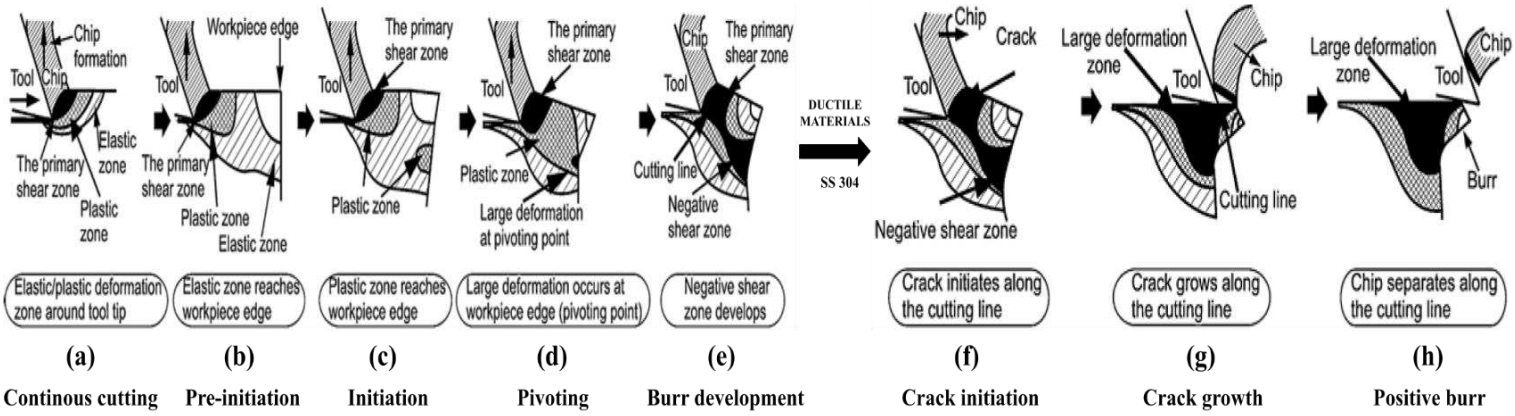

Fig. 10. Schematic burr formation [57]. (a) Continous cutting, (b) pre-initiation, (c) initiation, (d) pivoting, (e) burr development, (f) crack initiation, (g) crack growth, (h) positive burr.

This phenomenon becomes more pronounced in thin plates or under conditions of reduced structural rigidity, where additional deflection enlarges the large deformation zone and increases the tendency for edge folding [61] from a deformation-energy perspective, burr defects arise when the plastic energy accumulated in the shear zone is not fully released during chip separation. Local temperature increases under certain cutting conditions may reduce the yield strength of SS 304, thereby enlarging the volume of plastic deformation prior to fracture [62]. Consequently, burr height and morphology are governed by the interactions among material rigidity, local stress distribution, strain-hardening behaviour, and thermomechanical conditions within the cutting zone [63]. The schematic, therefore, confirms that, in SS 304, burr formation is a direct consequence of high ductility and deformation instability at the tool exit during milling [64].

4 Conclusions

This study demonstrates that the interactions among depth of cut, spindle speed, and material thickness significantly influence burr formation during the milling of thin SS 304 plates. An increase in depth of cut consistently leads to greater burr height due to intensified plastic deformation and lateral material flow at the tool exit. Spindle speed contributes through thermomechanical effects, which, under certain combinations, may either amplify or moderate burr intensity. Plates with a thickness of 1 mm exhibit the highest tendency towards deformation due to their lower structural rigidity, whereas 2 mm plates show a more stable response to cutting forces. These findings confirm that plate thickness functions as a structural rigidity factor governing edge deformation stability in ductile materials such as SS 304. Consequently, this study extends previous research, predominantly centred on bulk materials, by providing a

focused analysis of thin plates (1–2 mm) under conventional milling conditions. From a practical perspective, the combination of a spindle speed of 800 rpm and a depth of cut of 0.25 mm yields more controlled burr formation compared with other tested conditions. This outcome provides a practical guide to machining parameter selection to minimise burr defects without compromising process stability, while also establishing a more systematic understanding of burr formation trends in thin SS 304 plate applications.

References

[1] L. C. Silva and M. B. da Silva, "Investigation of burr formation and tool wear in micromilling operation of duplex stainless steel," *Precis. Eng.*, vol. 60, pp. 178–188, Nov. 2019, doi: 10.1016/j.precisioneng.2019.08.006.

[2] Q. Sun, X. Cheng, G. Zhao, X. Yang, and G. Zheng, "Experimental study of micromilling burrs of 304 stainless steel," *International Journal of Advanced Manufacturing Technology*, vol. 105, no. 11, pp. 4651–4662, Dec. 2019, doi: 10.1007/s00170-019-03839-3.

[3] R. Nakagawa, M. Fujimoto, and R. Tasaki, "Precision-enhanced deburring using machining force feedback control for various casting materials," *Mechanical Engineering Journal*, vol. 12, no. 3, pp. 24-00425-24–00425, 2025, doi: 10.1299/mej.24-00425.

[4] C. Liu, J. He, R. Lu, Z. Mo, H. Liu, and N. Yin, "Research on milling burrs of ALSI304 stainless steel with consideration of tool eccentricity," *Journal of Manufacturing and Materials Processing*, vol. 9, no. 12, Dec. 2025, doi: 10.3390/jmmp9120390.

[5] S. Senthil Kumar, K. Thirumavalavan, C. Kayelvizhi, and D. Sarukasan, "Performance and optimisation of AlCrN-coated cermet tools in machining SS 304 stainless steel," *Mater. Res. Express*, vol. 12, no. 8, Aug. 2025, doi: 10.1088/2053-1591/adf491.

[6] A. Siahsarani, M. Paknejad, and B. Azarhoushang, "Deburring of micro-milled hardened steel: influence of milling strategies and CNC-based post-polishing," *International Journal of Advanced Manufacturing Technology*, 2025, doi: 10.1007/s00170-025-16936-3.

[7] A. S. Ali, T. Abdelmonem, R. Elsoeudy, M. A. Mohsen, and N. Elzayady, "Characterisation of AISI 304 stainless steel based on laser cutting process optimisation," *Sci. Rep.*, vol. 15, no. 1, Dec. 2025, doi: 10.1038/s41598-025-24932-6.

[8] S. Hajiahmadi, "Burr size investigation in micro milling of stainless steel 316L," *International Journal of Lightweight Materials and Manufacture*, vol. 2, no. 4, pp. 296–304, Dec. 2019, doi: 10.1016/j.ijlmm.2019.07.004.

[9] Z. Kou, Y. Wan, Y. Cai, X. Liang, and Z. Liu, "Burr controlling in micro milling with supporting material method," in *Procedia Manufacturing*, Elsevier B.V., 2015, pp. 501–511. doi: 10.1016/j.promfg.2015.09.015.

[10] A. Siahsarani, M. Paknejad, and B. Azarhoushang, "Deburring of micro-milled hardened steel: influence of milling strategies and CNC-based post-polishing," *The International Journal of Advanced Manufacturing Technology*, Nov. 2025, doi: 10.1007/s00170-025-16936-3.

[11] P. Muthuswamy, "Investigation on sustainable machining characteristics of tools with serrated cutting edges in face milling of AISI 304 Stainless Steel," in *Procedia CIRP*, Elsevier B.V., 2022, pp. 865–871. doi: 10.1016/j.procir.2022.02.143.

[12] Z. Kou, Y. Wan, Y. Cai, X. Liang, and Z. Liu, "Burr controlling in micro milling with supporting material method," *Procedia Manuf.*, vol. 1, pp. 501–511, 2015, doi: 10.1016/j.promfg.2015.09.015.

[13] G.-L. Chern, "Study on mechanisms of burr formation and edge breakout near the exit of orthogonal cutting," *J. Mater. Process. Technol.*, vol. 176, no. 1–3, pp. 152–157, Jun. 2006, doi: 10.1016/j.jmatprotec.2006.03.127.

[14] F. Akkoyun, Z. A. Cevik, K. Ozsoy, A. Ercetin, and I. Arpaci, "Image processing approach to investigate the correlation between machining parameters and burr formation in micro-milling processes of selective-laser-melted AISI 316L," *Micromachines (Basel).*, vol. 14, no. 7, Jul. 2023, doi: 10.3390/mi14071376.

[15] A. Hrițuc, A. M. Mihalache, O. Dodun, L. Slătineanu, and G. Nagîț, "Evaluation of thin wall milling ability using disc cutters," *Micromachines (Basel).*, vol. 14, no. 2, p. 341, Jan. 2023, doi: 10.3390/mi14020341.

[16] M. Zawada-Michałowska, P. Pieśko, G. Mrówka-Nowotnik, A. Nowotnik, and S. Legutko, "Effect of the technological parameters of milling on residual stress in the surface layer of thin-walled plates," *Materials*, vol. 17, no. 5, Mar. 2024, doi: 10.3390/ma17051193.

[17] D. Cai, J. Li, N. Ren, H. Dong, and J. Li, "Interaction of MnS inclusion behaviors and macrosegregation during solidification by multi-phase modelling," *J. Mater. Process. Technol.*, vol. 297, p. 117243, Nov. 2021, doi: 10.1016/j.jmatprotec.2021.117243.

[18] P. Muthuswamy, "Investigation on sustainable machining characteristics of tools with serrated cutting edges in face milling of AISI 304 stainless steel," *Procedia CIRP*, vol. 105, pp. 865–871, 2022, doi: 10.1016/j.procir.2022.02.143.

[19] M. A. N. Rashid, T. Saleh, W. I. Noor, and M. S. M. Ali, "Effect of laser parameters on sequential laser beam micromachining and micro electro-discharge machining," Jan. 29, 2021. doi: 10.21203/rs.3.rs-170620/v1.

[20] C. Qu, W. Lu, H. Su, and M. Zhu, "Differences in yield behavior in the thickness direction of TMCP-processed hsla thick steel plates and the evolution of microstructure property gradients," *Metals (Basel).*, vol. 15, no. 11, p. 1229, Nov. 2025, doi: 10.3390/met15111229.

[21] B. Chandar J *et al.*, "Experimental analysis and optimisation of abrasive waterjet deep hole drilling process parameters for SS AISI 316L," *Journal of Materials Research and Technology*, vol. 26, pp. 7984–7997, Sep. 2023, doi: 10.1016/j.jmrt.2023.09.045.

[22] J. T. Toton Bsc, *Additively Manufactured Fe-25Co-15Mo Maraging Steel Cutting tools for aerospace machining via laser metal deposition*. 2022.

[23] C. Devanathan, R. Giri, C. Dinesh, and B. Gajesh, "Influence of process parameters on MRR and taper cut in micro drilling of SS304 using electrochemical machining," in *Materials Today: Proceedings*, Elsevier Ltd, 2020, pp. 3526–3532. doi: 10.1016/j.matpr.2020.11.1000.

[24] Q. Sun, X. Cheng, G. Zhao, X. Yang, and G. Zheng, "Experimental study of micromilling burrs of 304 stainless steel," *The International Journal of Advanced Manufacturing Technology*, vol. 105, no. 11, pp. 4651–4662, Dec. 2019, doi: 10.1007/s00170-019-03839-3.

[25] V. Venkatesh, N. Swain, G. Srinivas, P. Kumar, and H. C. Barshilia, "Review on the machining characteristics and research prospects of conventional microscale machining operations," Feb. 17, 2017, *Taylor and Francis Inc.* doi: 10.1080/10426914.2016.1151045.

[26] T. Wang, X. Wu, G. Zhang, B. Xu, Y. Chen, and S. Ruan, "Experimental study on machinability of zr-based bulk metallic glass during micro milling," *Micromachines (Basel).*, vol. 11, no. 1, Jan. 2020, doi: 10.3390/mi11010086.

[27] S. Tansukatanon, V. Tangwarodomnukun, C. Dumkum, P. Kruytong, N. Plaichum, and W. Charee, "Micromachining of stainless steel using TiAlN-coated tungsten carbide end mill," in *Procedia Manufacturing*, Elsevier B.V., 2019, pp. 419–426. doi: 10.1016/j.promfg.2019.02.058.

[28] J. Wang *et al.*, "Effect of alternating magnetic field intensity on microstructure and corrosion properties of deposited metal in 304 stainless steel TIG welding," *Metals (Basel).*, vol. 15, no. 7, Jul. 2025, doi: 10.3390/met15070761.

[29] T. Feldhausen, K. Saleeby, and T. Kurfess, "Spinning the digital thread with hybrid manufacturing," *Manuf. Lett.*, vol. 29, pp. 15–18, Aug. 2021, doi: 10.1016/j.mfglet.2021.05.003.
[30] X. Xu, Z. Xie, M. Wu, and C. Ma, "Effects of laser process parameters on melt pool thermodynamics, surface morphology and residual stress of laser powder bed-fused TiAl-based composites," 2025, doi: 10.3390/met15111234.
[31] G. U. Rehman, M. R. ul Haq, M. Masud, S. H. I. Jaffery, M. S. Khan, and S. I. Butt, "Statistical analysis of burr width and height in conventional speed micro-milling of titanium alloy (Ti-6Al-4V) by varying cutting parameters under different lubrication methods: Dry, MQL and wet," in *ICAME 2025*, Basel Switzerland: MDPI, Oct. 2025, p. 11. doi: 10.3390/engproc2025111011.
[32] D. O'Sullivan and M. Cotterell, "Machinability of austenitic stainless steel SS303," *J. Mater. Process. Technol.*, vol. 124, no. 1–2, pp. 153–159, Jun. 2002, doi: 10.1016/S0924-0136(02)00197-8.
[33] A. W. Tehami, M. R. ul Haq, M. A. Khan, S. H. I. Jaffery, M. I. Faraz, and J. Petru, "Comparative evaluation of burr formation in low-speed, high-speed and novel laser hybrid high-speed micromilling of Inconel 718," *Journal of Materials Research and Technology*, vol. 41, pp. 5188–5204, Mar. 2026, doi: 10.1016/j.jmrt.2026.02.071.
[34] S. P. F. C. Jaspers and J. H. Dautzenberg, "Material behaviour in conditions similar to metal cutting: flow stress in the primary shear zone," *J. Mater. Process. Technol.*, vol. 122, no. 2–3, pp. 322–330, Mar. 2002, doi: 10.1016/S0924-0136(01)01228-6.
[35] A. S. Ali, T. Abdelmonem, R. Elsoeudy, M. A. Mohsen, and N. Elzayady, "Characterisation of AISI 304 stainless steel based on laser cutting process optimisation," *Sci. Rep.*, vol. 15, no. 1, p. 41036, Nov. 2025, doi: 10.1038/s41598-025-24932-6.
[36] B. Chandar J *et al.*, "Experimental analysis and optimisation of abrasive waterjet deep hole drilling process parameters for SS AISI 316L," *Journal of Materials Research and Technology*, vol. 26, pp. 7984–7997, Sep. 2023, doi: 10.1016/j.jmrt.2023.09.045.
[37] F. Akkoyun, Z. A. Cevik, K. Ozsoy, A. Ercetin, and I. Arpaci, "Image processing approach to investigate the correlation between machining parameters and burr formation in micro-milling processes of selective-laser-melted AISI 316L," *Micromachines (Basel).*, vol. 14, no. 7, p. 1376, Jul. 2023, doi: 10.3390/mi14071376.
[38] N. Kong, J. Zhang, H. Li, B. Wei, and D. R. G. Mitchell, "The influence of a novel inorganic-polymer lubricant on the microstructure of interstitial-free steel during ferrite rolling," *Metals (Basel).*, vol. 10, no. 2, p. 178, Jan. 2020, doi: 10.3390/met10020178.
[39] S.-T. Hong, Y.-F. Li, J.-W. Park, and H. N. Han, "Effectiveness of electrically assisted solid-state pressure joining using an additive manufactured porous interlayer," *CIRP Annals*, vol. 67, no. 1, pp. 297–300, 2018, doi: 10.1016/j.cirp.2018.04.062.
[40] F. Z. Fang, X. D. Zhang, W. Gao, Y. B. Guo, G. Byrne, and H. N. Hansen, "Nanomanufacturing—Perspective and applications," *CIRP Annals*, vol. 66, no. 2, pp. 683–705, 2017, doi: 10.1016/j.cirp.2017.05.004.
[41] A. G. dos Santos, M. B. da Silva, and M. J. Jackson, "Investigations on burr formation mechanisms and surface quality when micro-milling duplex stainless steel (UNS S32205)," *Journal of Micromanufacturing*, Jun. 2023, doi: 10.1177/25165984231173186.
[42] R. Nakagawa, M. Fujimoto, and R. Tasaki, "Precision-enhanced deburring using machining force feedback control for various casting materials," *Mechanical Engineering Journal*, vol. 12, no. 3, pp. 24–00425, 2025, doi: 10.1299/mej.24-00425.
[43] T. Wang, X. Wu, G. Zhang, B. Xu, Y. Chen, and S. Ruan, "Experimental study on machinability of zr-based bulk metallic glass during micro milling," *Micromachines (Basel).*, vol. 11, no. 1, p. 86, Jan. 2020, doi: 10.3390/mi11010086.
[44] S. Senthil Kumar, K. Thirumavalavan, C. Kayelvizhi, and D. Sarukasan, "Performance and optimisation of AlCrN-coated cermet tools in machining SS 304 stainless steel," *Mater. Res. Express*, vol. 12, no. 8, p. 086506, Aug. 2025, doi: 10.1088/2053-1591/adf491.
[45] A. Hrițuc, A. M. Mihalache, O. Dodun, L. Slătineanu, and G. Nagîț, "Evaluation of thin wall milling ability using disc cutters," *Micromachines (Basel).*, vol. 14, no. 2, p. 341, Jan. 2023, doi: 10.3390/mi14020341.
[46] C. Liu, J. He, R. Lu, Z. Mo, H. Liu, and N. Yin, "Research on milling burrs of ALSI304 stainless steel with consideration of tool eccentricity," *Journal of Manufacturing and Materials Processing*, vol. 9, no. 12, p. 390, Nov. 2025, doi: 10.3390/jmmp9120390.
[47] S. Senthil Kumar, K. Thirumavalavan, C. Kayelvizhi, and D. Sarukasan, "Performance and optimisation of AlCrN-coated cermet tools in machining SS 304 stainless steel," *Mater. Res. Express*, vol. 12, no. 8, p. 086506, Aug. 2025, doi: 10.1088/2053-1591/adf491.
[48] Z. Wen, G. Wang, and M. Li, "Surface morphology, burr formation, and spindle axial drift in high-speed robotic milling of complex features," *Proc. Inst. Mech. Eng. B J. Eng. Manuf.*, vol. 239, no. 8, pp. 1152–1165, Jun. 2025, doi: 10.1177/09544054241254890.
[49] D. Mai, B. C. Kwon, and S. L. Ko, "Practical implementation of cutting force model for step drill using 3D CAD data," *CIRP Annals*, vol. 68, no. 1, pp. 85–88, 2019, doi: 10.1016/j.cirp.2019.04.055.
[50] R. Nishida, J. Zhong, and T. Shinshi, "Forced liquid cooling of piezoelectric stack actuator utilising silicone oil," *Precis. Eng.*, vol. 75, pp. 120–128, May 2022, doi: 10.1016/j.precisioneng.2022.01.012.
[51] D. Cai, J. Li, N. Ren, H. Dong, and J. Li, "Interaction of MnS inclusion behaviors and macrosegregation during solidification by multi-phase modelling," *J. Mater. Process. Technol.*, vol. 297, p. 117243, Nov. 2021, doi: 10.1016/j.jmatprotec.2021.117243.
[52] B. Chen, X. Guan, D. Cai, and H. Li, "Simulation on thermal characteristics of high-speed motorised spindle," *Case Studies in Thermal Engineering*, vol. 35, p. 102144, Jul. 2022, doi: 10.1016/j.csite.2022.102144.
[53] S. H. Lee and S.-H. Lee, "Optimisation of cutting parameters for burr minimisation in face-milling operations," *Int. J. Prod. Res.*, vol. 41, no. 3, pp. 497–511, Jan. 2003, doi: 10.1080/0020754021000042382.
[54] C. Ma, J. Yang, L. Zhao, X. Mei, and H. Shi, "Simulation and experimental study on the thermally induced deformations of high-speed spindle system," *Appl. Therm. Eng.*, vol. 86, pp. 251–268, Jul. 2015, doi: 10.1016/j.applthermaleng.2015.04.064.
[55] V. N. Gaitonde, S. R. Karnik, and J. P. Davim, "Minimising burr size in drilling: integrating response surface methodology with particle swarm optimisation," in *Mechatronics and Manufacturing Engineering*, Elsevier, 2012, pp. 259–292. doi: 10.1533/9780857095893.259.
[56] S. Tansukatanon, V. Tangwarodomnukun, C. Dumkum, P. Kruytong, N. Plaichum, and W. Charee, "Micromachining of stainless steel using TiAlN-coated tungsten carbide end mill," *Procedia Manuf.*, vol. 30, pp. 419–426, 2019, doi: 10.1016/j.promfg.2019.02.058.
[57] J. C. Aurich, D. Dornfeld, P. J. Arrazola, V. Franke, L. Leitz, and S. Min, "Burrs-Analysis, control and removal," *CIRP Ann. Manuf. Technol.*, vol. 58, no. 2, pp. 519–542, 2009, doi: 10.1016/j.cirp.2009.09.004.
[58] S. Y. Jin, A. Pramanik, A. K. Basak, C. Prakash, S. Shankar, and S. Debnath, "Burr formation and its treatments—a review," Mar. 01, 2020, *Springer*. doi: 10.1007/s00170-020-05203-2.

[59] G. A. Student David Dornfeld Professor MemASME, "Sung-Lim Ko A study on burr formation mechanism," 1991. [Online]. Available: http://www.asme.org/about-asme/terms-of-use
[60] W. Wu, J. Dai, L. Chen, D. Liu, and X. Zhou, "Experiment analysis on crack resistance in negative moment zone of steel–concrete composite continuous girder improved by interfacial slip," *Materials*, vol. 15, no. 23, p. 8319, Nov. 2022, doi: 10.3390/ma15238319.
[61] H. Zhang, X. Liu, and W. Yi, "Experimental investigation on stress redistribution and load-transfer paths of shear walls with openings," *Journal of Structural Engineering*, vol. 144, no. 9, Sep. 2018, doi: 10.1061/(ASCE)ST.1943-541X.0002110.
[62] S. A. Niknam and V. Songmene, "Milling burr formation, modeling and control: A review," Jun. 01, 2015, *SAGE Publications Ltd*. doi: 10.1177/0954405414534827.
[63] V. Seriacopi, N. K. Fukumasu, R. M. Souza, and I. F. Machado, "Finite element analysis of the effects of thermo-mechanical loadings on a tool steel microstructure," *Eng. Fail. Anal.*, vol. 97, pp. 383–398, Mar. 2019, doi: 10.1016/j.engfailanal.2019.01.006.
[64] F. Z. Fang and Y. C. Liu, "On minimum exit-burr in micro cutting," *Journal of Micromechanics and Microengineering*, vol. 14, no. 7, pp. 984–988, Jul. 2004, doi: 10.1088/0960-1317/14/7/020.